Neuropharmacology 73 (2013) 388–396

Contents lists available at SciVerse ScienceDirect

Neuropharmacology

journal homepage: www.elsevier.com/locate/neuropharm

Synaptic plasticity alterations associated with memory impairment induced by deletion of CB2 cannabinoid receptors

María S. García-Gutiérrez [a,d,1], Antonio Ortega-Álvaro [b,c,1], Arnau Busquets-García [c], Jose M. Pérez-Ortiz [b], Laura Caltana [e], María Jimena Ricatti [e], Alicia Brusco [e], Rafael Maldonado [c], Jorge Manzanares [a,d,*]

[a] Instituto de Neurociencias, Campus de San Juan, Universidad Miguel Hernández-CSIC, San Juan de Alicante, Alicante, Spain
[b] Unidad de Neuropsicofarmacología Traslacional, Complejo Hospitalario Universitario de Albacete, C/ Hermanos Falcó 37, Albacete, Spain
[c] Laboratori de Neurofarmacología, Universitat Pompeu Fabra, Barcelona, Spain
[d] Red Temática de Investigación Cooperativa en Salud (RETICS), Red de Trastornos Adictivos, Instituto de Salud Carlos III, MICINN and FEDER, Madrid, Spain
[e] Instituto de Biología Celular y Neurociencia "Prof. E. De Robertis" (UBA-CONICET), Buenos Aires, Argentina

ARTICLE INFO

Article history:
Received 7 January 2013
Received in revised form
15 May 2013
Accepted 17 May 2013

Keywords:
CB_2r
Mice lacking CB_2r
Memory
Cannabinoid CB_2r-agonist JWH133
Immunohistochemistry
Rt-PCR

ABSTRACT

In this study, the role of CB_2r on aversive memory consolidation was further evaluated. Mice lacking CB_2r (CB2KO) and their corresponding littermates (WT) were exposed to the step-down inhibitory avoidance test (SDIA). MAP2, NF200 and synaptophysin (SYN)-immunoreactive fibers were studied in the hippocampus (HIP) of both genotypes. The number of synapses, postsynaptic density thickness and the relation between the synaptic length across the synaptic cleft and the distance between the synaptic ends were evaluated in the HIP (dentate gyrus (DG) and CA1 fields) by electron microscopy. Brain-derived neurotrophic factor (BDNF), glucocorticoid receptor (NR3C1) gene expressions and mTOR/p70S6K signaling cascade were evaluated in the HIP and prefrontal cortex (PFC). Finally, the effects of acute administration of CB_2r-agonist JWH133 or CB_2r-antagonist AM630 on memory consolidation were evaluated in WT mice by using the SDIA.

The lack of CB_2r impaired aversive memory consolidation, reduced MAP2, NF200 and SYN-immunoreactive fibers and also reduced the number of synapses in DG of CB2KO mice. BDNF and NR3C1 gene expression were reduced in the HIP of CB2KO mice. An increase of p-p70S6K (T389 and S424) and p-AKT protein expression was observed in the HIP and PFC of CB2KO mice. Interestingly, administration of AM630 impaired aversive memory consolidation, whereas JWH133 enhanced it. Further functional and molecular assessments would have been helpful to further support our conclusions.

These results revealed that CB_2r are involved in memory consolidation, suggesting that this receptor could be a promising target for developing novel treatments for different cognitive impairment-related disorders.

1. Introduction

Over the last few years, the endocannabinoid system (ECS) has emerged as a neuromodulatory system involved in different processes such as stress, anxiety, depression, drug addiction and memory (Urigüen et al., 2004; Puighermanal et al., 2009). Most of these studies focused on the role of cannabinoid CB1 receptors (CB_1r) due to their wide distribution in human and rodent brains (Herkenham et al., 1991). The presence of a high density of CB_1r in the brain areas which regulate learning and memory, such as the hippocampus (HIP), suggested the potential role of this receptor in cognitive behavior. Different animal models have been used extensively to evaluate the function of CB_1r in various states of learning and memory, including acquisition, consolidation and retrieval (Riedel and Davies, 2005). CB_1r-agonists impair working memory and the acquisition of long-term memory (Costanzi et al., 2004; Mishima et al., 2001). The fact that these effects were

* Corresponding author. Instituto de Neurociencias de Alicante, Universidad Miguel Hernández-CSIC, Apartado de correos 18, 03550 San Juan de Alicante, Spain. Tel.: +34 96 591 9248.
E-mail addresses: jmanzanares@umh.es, jmanzanares6@terra.es (J. Manzanares).
[1] Both authors have equally contributed to the manuscript.

0028-3908/$ – see front matter © 2013 Elsevier Ltd. All rights reserved.
http://dx.doi.org/10.1016/j.neuropharm.2013.05.034

blocked by the administration of CB_1r-antagonist, SR141716A, supports CB_1r as being the target involved in the acute effects of cannabinoids on memory impairments (Da and Takahashi, 2002; Pamplona and Takahashi, 2006). Interestingly, pharmacological or genetic disruption of CB_1r signaling enhances learning and memory in a variety of spatial and operant paradigms (Thiemann et al., 2007). Further studies revealed the modulation of GABA neurotransmission through the activation of CB_1r located on GABA interneurons, the indirect activation of the mammalian target of rapamycin (mTOR)/70-kDa ribosomal protein S6 kinase (p70S6K) signaling cascade and NMDA receptors as the main mechanisms underlying the cognitive impairments produced by cannabinoids (Puighermanal et al., 2009). In contrast, the fact that a number of effects mediated by cannabinoids persisted in mice lacking the CB_1r (CB1KO) pointed to the involvement of additional cannabinoid receptors (Breivogel et al., 2001; Hajos et al., 2001; Kofalvi et al., 2003).

Cannabinoid CB_2 receptors (CB_2r) is expressed in several brain regions including the HIP, cerebral cortex, amygdala, striatum, thalamus and cerebellum (Gong et al., 2006; García-Gutiérrez et al., 2010). In contrast, some studies found a lack of specific CB_2 binding and lack of CB_2 mRNA in the rat brain (Griffin et al., 1999). One possible explanation for this controversy is based on the lack of specificity of the available CB_2r antibodies (Atwood and Mackie, 2010; Baek et al., 2013).

Nevertheless, several evidences supported the potential functional effects of CB_2r in several brain regions (Van Sickle et al., 2005; Onaivi et al., 2008; Morgan et al., 2009; García-Gutiérrez et al., 2010; Xi et al., 2011; García-Gutiérrez and Manzanares, 2011; Ortega-Álvaro et al., 2011; Aracil-Fernández et al., 2012;). Transgenic mice overexpressing CB_2r in the central nervous system (CB2xP) exhibited a clear endophenotype resistance to anxiogenic (García-Gutiérrez and Manzanares, 2011) and depressogenic-like (García-Gutiérrez et al., 2010) stimuli associated with molecular adaptations in different key elements, such as the hypothalamic–pituitary–adrenal (HPA) axis (García-Gutiérrez and Manzanares, 2011), neurotrophic factors (García-Gutiérrez et al., 2010) and the GABAergic system (García-Gutiérrez and Manzanares, 2011). Interestingly, deletion of the CB_2r gene produced behavioral alterations that are commonly expressed in preclinical animal models of schizophrenia, namely altered locomotor activity, anxiety-like and depressive-like behaviors and cognitive deficits, including impaired sensorimotor gating (Ortega-Álvaro et al., 2011).

The high expression of CB_2r in areas involved in learning and memory, such as the HIP, the close interaction between CB_2r and the GABAergic system and the cognitive alterations observed in CB2KO mice, suggests that CB_2r might be an important neurobiological substrate for cognitive processes. In the present study, we further investigated the specific function of CB_2r in learning and memory. CB2KO mice were exposed to the step-down inhibitory avoidance test (SDIA). Immunohistological analyses of MAP2, NF200 and synaptophysin (SYN) were studied in the dentate gyrus (DG) and CA1 fields of the HIP of CB2KO and WT mice. In addition, brain-derived neurotrophic factor (BDNF) and glucocorticoid receptor (NR3C1) gene expression were analyzed in the HIP of both genotypes. The protein expression of the phosphorylated p-p70S6K, the phosphorylated protein kinase B (pAKT) and the phosphorylated ribosomal protein S6 (P-S6) in the HIP and prefrontal cortex (PFC) of CB2KO were studied to establish the possible involvement of the phosphatidylinositol-3 kinase (PI3K)/mTOR pathway in the cognitive impairment produced by the deletion of CB_2r. Finally, the effects of the cannabinoid CB_2r-agonist JWH133 or cannabinoid CB_2r-antagonist AM630 on memory consolidation were evaluated in WT mice by using the SDIA.

2. Material and methods

2.1. Animals

Male mice lacking CB_2r (CB2KO) and their corresponding wild-type (WT) littermates were used in all of the experiments. All mice were born in our animal facilities from breeding pairs of CB2±. CB2KO founders on a C57BL/6J congenic background (kindly provided by Nancy E. Buckley, Cal State Polytechnic Univ., Pomona, CA, USA) were crossed with an outbred CD1 (Charles River, France) background. Heterozygote sixth generation mice were bred on a CD1 background at our animal vivarium and homozygotes from the same generation were selected for our experiments. In all the experiments, the mice used were matched for age (2–3 months old) and weight (25–35 g), and were kept in controlled temperature (23 ± 2 °C) and light conditions (light–dark cycle switching at 8:00 a.m. and 8:00 p.m.) with free access to food (commercial diet for rodents A04 Panlab, Barcelona, Spain) and water. All the experiments were carried out between 9.00 and 13.00 h. All studies were performed in compliance with the Royal Decree 223/1998 of 14 March (BOE. 8 18) and the Ministerial Order of 13 October 1989 (BOE 18) as well as with the European Council Directive of 24 November 1986 (86/609/EEC).

2.2. Drugs

The CB_2r-antagonist AM630 (6-Iodo-2-methyl-1-[2-(4-morpholinyl) ethyl]-1Hindol-3-yl](4-methoxyphenyl)methanone) (Pertwee et al., 1995) and the CB_2r-agonist JWH133 ((6aR,10aR)-3-(1,1-Dimethylbutyl)-6a,7,10,10a-tetrahydro-6,6,9-trimethyl-6H-dibenzo[b,d]pyran) (Huffman et al., 1999) were obtained from Tocris (Biogen, Madrid, Spain) and dissolved in DMSO: Tween 80: distilled water (1:1:8) immediately before use. AM630 (1, 2 or 3 mg kg^{-1}; 0.3 ml; i.p.) or JWH133 (0.5, 1 or 2 mg kg^{-1}; 0.3 ml; i.p.) were administered immediately after mice received a scrambled foot shock (0.5 mA, 2 s) in the SDIA pretraining session.

2.3. Step-down inhibitory avoidance test (SDIA)

The SDIA apparatus was a 50 × 25 × 25 cm acrylic box with a floor consisting of a grid of parallel stainless steel bars, 1 mm in diameter and 1 cm apart. A 10 cm^2 wide, 2 cm high acrylic platform was placed in the corner of the floor. Animals were placed on the platform. Immediately upon stepping down, mice received a scrambled foot shock (0.5 mA for 2 s), and, they were then withdrawn from the apparatus. In pharmacological studies, mice received JWH133 (0.5, 1 or 2 mg kg^{-1}; 0.3 ml; i.p.) or AM630 (0.5, 1 or 2 mg kg^{-1}; 0.3 ml; i.p.) after receiving the scrambled foot shock. In the retention sessions, 1 and 24 h after, no foot shock was administered and the step-down latency (to a ceiling of 180 s) was used as a measure of retention. At 24 h, long-term memory (LTM) is well established and, consequently cognitive deficits, including short (1 h) term memory, are scored with this test.

2.4. Immunohistochemistry analyses

CB2KO and WT mice (n = 3–5/group) were anesthetized (ketamine/xylazine; 88 mg kg^{-1}/44 mg kg^{-1}, 2:1 v/v, 0.2 ml, i.p), and intracardially perfused with 4% paraformaldehyde in phosphate buffer (PB; 0.1 M, pH 7.4). Brains were dissected, postfixed overnight at 4 °C, frozen and cut into coronal 50-μm sections using a vibratome. Vibratome brain sections of CB2KO and WT mice containing DG and CA1 areas were simultaneously processed as described previously (Caltana et al., 2009). Briefly, sections were rinsed in phosphate-buffered saline (PBS) and endogenous peroxidase activity was inhibited with 0.5% (v/v) H_2O_2 in PBS for 30 min at room temperature (RT). Brain sections were then blocked for 1 h with 3% (v/v) normal goat serum in PBS and were incubated for 24 h at 4 °C with the primary antibodies: mouse anti-MAP2 (Sigma; 1:1000), mouse anti-NF200 (Sigma; 1:3000), and mouse anti-SYN (Sigma; 1:1000). They were then rinsed and incubated for 1 h at RT with biotinylated secondary antibodies (Sigma; 1:500). After further washing in PBS, sections were incubated for 1 h with Extravidin complex solution (1:500). After washing in PBS (×3) and in acetate buffer (×2) (0.1 M, pH 6), the development of peroxidase activity was carried out with 0.035% (w/v) 3,30-diaminobenzidine plus 2.5% (w/v) nickel ammonium sulfate and 0.1% (v/v) H_2O_2 dissolved in acetate buffer. Subsequently, sections were washed with distilled water, dehydrated, and coverslipped using Permount.

2.5. Morphometric digital image analysis

Measurements of CB2KO and WT sections were carried out under standardized conditions (in the same session, on the same day). In each tissue section, each microscopic field was selected within the limits of each anatomical area of interest to be morphometrically analyzed. Tissue images were obtained through an Axiolab Zeiss light microscope equipped with a cooled-digital camera Olympus QColor3.

In order to evaluate the MAP2 and NF200-inmunoreactive (ir) fibers, the total area of the immunolabeled fibers was related to the total area of the corresponding microscopic field (20× primary magnification), thus rendering a relative area parameter. Relative optical density (ROD) of SYN-ir structures was obtained after a

transformation of mean gray values into ROD by using the formula: ROD = log (256/mean gray). A background parameter was obtained from each section from the labeled structures and subtracted to each ROD cell before statistically processing values (Tagliaferro et al., 2006).

Electron microscopy photographs were digitally processed in order to count the number of synapses, and to measure postsynaptic density thickness as well as the relation between the synaptic length across the synaptic cleft and the distance between the synaptic ends, using Image Pro Software. Postsynaptic density thickness was evaluated as the length of a perpendicular line traced from the postsynaptic membrane to the most convex part of the synaptic complex in 20,000× primary magnification EM photographs (Tagliaferro et al., 2006).

2.6. Electron microscopy studies

After perfusion, CB2KO and WT dissected brain sections of 1 mm^3 corresponding to the DG and CA1 areas were postfixed in 1% osmium tetroxide in phosphate buffer 0.1 M for 30 min. After dehydration in graded ethanol, tissues were contrasted with 5% uranyl acetate and then embedded in Durcupan (Fluka AG, Chemische Fabrik, Buchs SG, Switzerland). Ultrathin sections were stained with lead citrate (standard method according to Reynolds) (Reynolds, 1963), and then observed and photographed with a Zeiss 109 electron microscope equipped with a GATAN digital camera.

2.7. Western blot

Frozen hippocampal tissues were processed as previously reported (Puighermanal et al., 2009). The antibodies used for immunoblot were: anti-phospho-p70S6K (T389) (1:400), anti-phosho-p70S6K (S424) (1:200), anti-p70S6K (1:500), anti-phosho-S6 (S235/236) (1:1200), anti-phosho-S6 (S240) (1:1000) obtained from Cell Signaling (Beverly, MA, USA); anti-phospho-AKT (S473) (1:5000) obtained from Sigma (Madrid, Spain); anti-glyceraldehyde-3-phosphate dehydrogenase (GAPDH) (1:5000) obtained from Santa Cruz Biotechnology (Santa Cruz, CA, USA). Optical densities of the relevant immunoreactive bands were quantified after acquisition on a ChemiDoc XRS System (Bio-Rad, Hercules, CA, USA) controlled by Quantity One software v 4.6.3 (Bio-Rad).

2.8. Rt-PCR analyses

Brain derived neurotrophic factor (BDNF) and glucocorticoid receptor (NR3C1) gene expression were examined by real time PCR (Rt-PCR) in the HIP of CB2KO and WT mice. Briefly, mice were killed and brains were removed from the skull and frozen over dry ice. Brain sections (500 μm) were cut at different levels containing the HIP (figure 20, 1.34 mm from bregma) (Paxinos and Franklin, 2001), mounted onto slides and stored at −80 °C. Sections were dissected following the method described by Palkovits (Palkovits, 1983). Total RNA was obtained from brain punches using Biozol® Total RNA extraction reagent (Bioflux, Inilab, Madrid, Spain). The reverse transcription was carried out following the manufacturer's instructions (Epicentre, Tech. Corp., Madison, Wisconsin). BDNF and NR3C1 gene expression were measured by using Taqman® Gene Expression assays (Mm00432069_m1 and Mm 00438286_m1, respectively) (Applied Biosystems, Madrid, Spain) as a double-stranded DNA-specific fluorescent dye and performed on the AbbiPrism 7700 Real Time Cycler (Applied Biosystems, Madrid, Spain). The reference gene used was 18S rRNA, detected using Taqman® ribosomal RNA control reagents. All primer–probe combinations were optimized and validated for the relative quantification of gene expression. Briefly, data for each target gene were normalized to the endogenous reference gene, and the fold change in target gene abundance was determined using the $2^{-\Delta\Delta Cr}$ method (Livak and Schmittgen, 2001).

2.9. Statistical analyses

Statistical analyses were performed using Student *t*-test or two-way analysis of variance followed by the Student Newman Keuls test when comparing two or four groups, respectively. Differences were considered significant if error probability was less than 5%. Data are presented as mean ± S.E.M. SigmaStat 3.1 software was used for all statistical analyses.

3. Results

3.1. Basal step-down inhibitory avoidance test

The results revealed that WT mice presented a significant increased latency at 1 and 24 h compared with their control group (training). Interestingly, no difference was observed in CB2KO mice at 1 and 24 h compared with their control group (training). Indeed, CB2KO presented a reduced latency compared with WT mice at training −1 and 24 h sessions (Two way ANOVA followed by Student Newman Keuls test: genotype $F_{(1,59)} = 55.298$, $p < 0.001$; time $F_{(2,59)} = 18.270$, $p < 0.001$; genotype × time $F_{(2,59)} = 18.498$, $p < 0.001$) ($n = 10$/group) (Fig. 1).

3.2. Immunohistochemistry analyses: MAP2, NF200 and SYN protein expression

The results revealed that CB2KO presented a significant reduction in MAP2 (Student's Newman–Keuls test, $t = 6.334$, $p < 0.001$, 10df) ($n = 6$/group) (Fig. 2A andB) and NF200 in DG compared with WT mice (Student's Newman–Keuls test, $t = 3.758$, $p = 0.004$, 10df) ($n = 6$/group) (Fig. 2C and D). However, no significant difference between CB_2KO and WT was observed in either MAP2 (Student's Newman–Keuls test, $t = -0.876$, $p = 0.402$, 10df) ($n = 6$/group) (Fig. 2A and B) or NF200 immunostaining in CA1 (Student's Newman–Keuls test, $t = -0.802$, $p = 0.441$, 10df) ($n = 6$/group) (Fig. 2C and D).

Indeed, the results revealed that the pattern of the SYN expression was significantly lower in CB2KO mice compared with WT mice in DG (Student's Newman–Keuls test, $t = 4.700$, $p < 0.001$, 10df) ($n = 6$/group) (Fig. 2E and F). However, no difference was observed in the CA1 region (Student's Newman–Keuls test, $t = 3.525$, $p = 0.005$, 10df) ($n = 6$/group) (Fig. 2E and F).

3.3. Electron microscopy studies

The electron microscopy study showed a significant reduction in the number of synapses in DG (Student's Newman–Keuls test, $t = 4.378$, $p < 0.001$, 12df) ($n = 7$/group) (Fig. 3A) and CA1 (Student's Newman–Keuls test, $t = 2.468$, $p = 0.043$, 7df) ($n = 4$–6/group) (Fig. 3B). However, there were no ultrastructural differences between CB2KO and WT mice. The synapses presented the classical ultrastructural components such as synaptic vesicles and mitochondria at the presynaptic terminal in DG (Student's Newman–Keuls test, $t = 0.936$, $p = 0.385$, 6df) ($n = 3$–6/group) (Fig. 3C) and CA1 (Student's Newman–Keuls test, $t = 0.906$, $p = 0.402$, 7df) ($n = 3$–6/group) (Fig. 3D). No difference was observed in the postsynaptic densities or cleft morphology in any of the regions analyzed (DG: Student's Newman–Keuls test, $t = -1.636$, $p = 0.177$, 4df; Fig. 3E) (CA1: Student's Newman–Keuls test, $t = -0.0889$, $p = 0.933$, 4df; Fig. 3F).

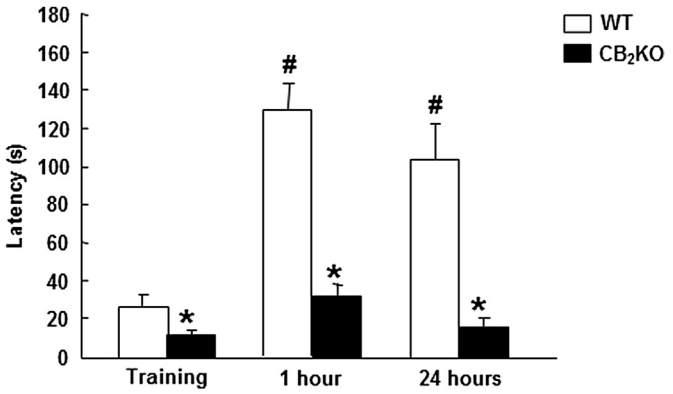

Fig. 1. Step-down inhibitory avoidance test (SDIA). CB2KO and their corresponding littermates WT mice were exposed to a scrambled foot shock (0.5 mA for 2 s) and the step-down latency(s) was measured 1 h (short-term memory) and 24 h later (long-term memory). Columns represent the mean and vertical lines ± S.E.M of step-down latency(s). #, values that are significantly difference ($p < 0.05$) from their corresponding controlgroup (training WT). *, values of CB2KO mice that are significantly ($p < 0.05$) different from their corresponding WT control group.

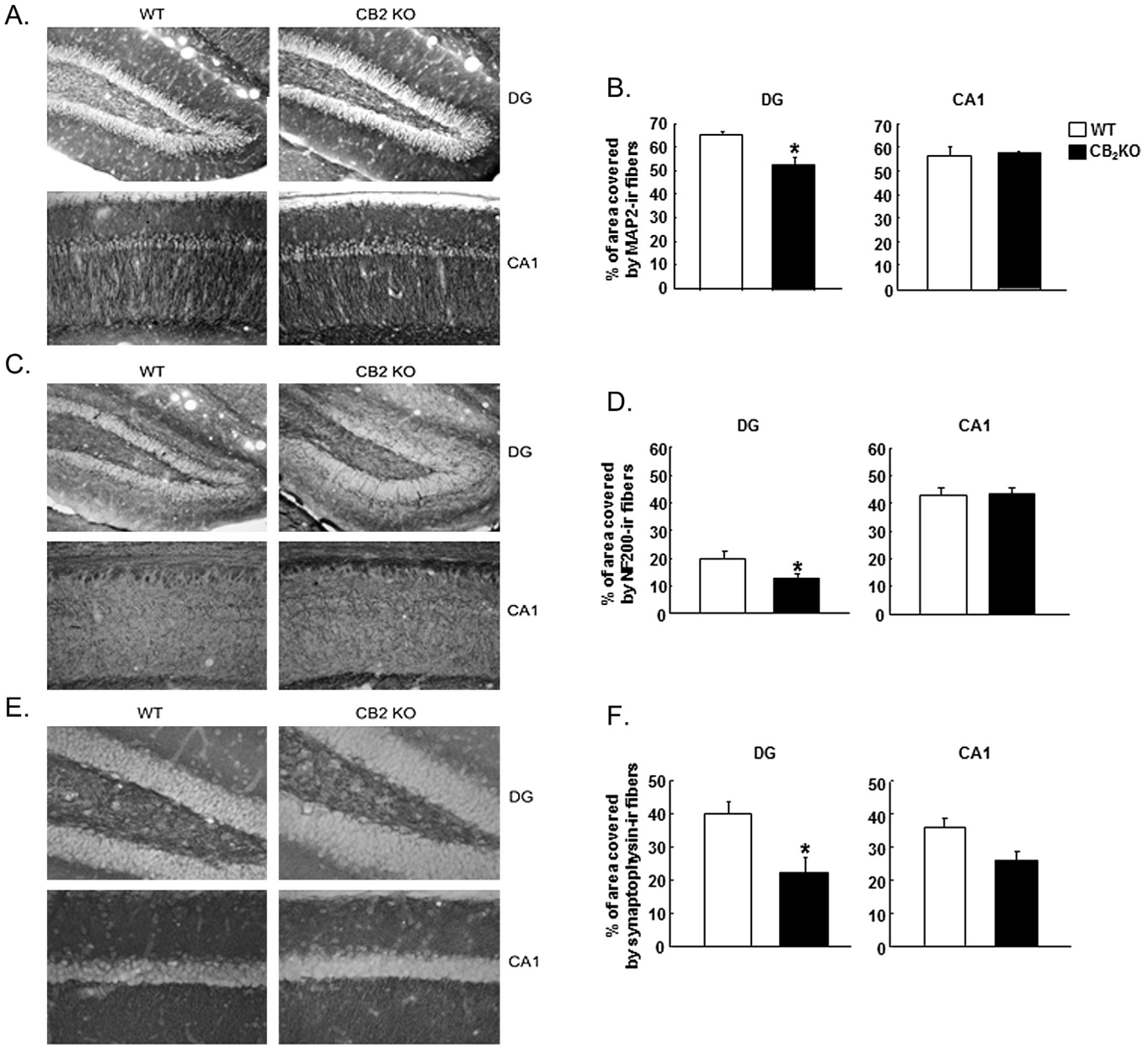

Fig. 2. MAP2, NF200 and SYN immunostaining in the DG and CA1 fields of the HIP of CB2KO and WT mice. Immunohistochemistry and densitometric analysis of MAP2 (A, B), NF200 (C, D) and SYN (E, F) in the DG and CA1 from CB2KO and WT mice. Columns represent the mean and vertical lines ± S.E.M of % of area covered by immunoreactive (ir) fibers. *, Values that are significantly ($p < 0.05$) different from their control group. Images are representative of several slices. Scale bars are included in each image.

3.4. Rt-PCR analyses: BDNF and NR3C1 gene expression in the HIP of CB2KO and WT

A significant reduction of BDNF (50%) was observed in the HIP of CB2KO compared with WT mice (Student's Newman–Keuls test, $t = 4.334$, $p < 0.001$, 12df) ($n = 6–8$/group) (Fig. 4A). Interestingly, CB2KO presented reduced NR3C1 gene expression (23.7%) in the HIP compared with WT mice (Student's Newman–Keuls test, $t = 2.343$, $p = 0.036$, 13df) ($n = 6–8$/group) (Fig. 4B).

3.5. mTOR signaling cascade: hippocampus and prefrontal cortex

The phosphorylation of p70S6K (T389), p70S6K (S424) and AKT was significantly increased in the PFC (Student's Newman–Keuls test, $t = -5.312$, $p < 0.001$, 12df (Fig. 4C); Student's Newman–Keuls test, $t = -4.462$, $p < 0.001$, 11df (Fig. 4D); Student's Newman–Keuls test, $t = -2.892$, $p = 0.016$, 10df (Fig. 4E), respectively) and the HIP of CB2KO compared with WT mice (Student's Newman–Keuls test, $t = -4.317$, $p = 0.001$, 11df (Fig. 4H); Student's Newman–Keuls test, $t = -5.730$, $p < 0.001$, 10df (Fig. 4I); Student's Newman–Keuls test, $t = -5.434$, $p < 0.001$, 12df (Fig. 4J), respectively). In contrast, no difference was observed in the phosphorylation of p-S6 (S235/236) or p-S6 (S240) between both genotypes at either of the regions analyzed (PFC: Student's Newman–Keuls test, $t = 1.144$, $p = 0.277$, 11df (Fig. 4F); Student's Newman–Keuls test, $t = -1.648$, $p = 0.128$, 11df (Fig. 4G)) (HIP: Student's Newman–Keuls test, $t = 1.198$, $p = 0.256$, 11df (Fig. 4K); Student's Newman–Keuls test, $t = 0.560$, $p = 0.587$, 11df (Fig. 4L)).

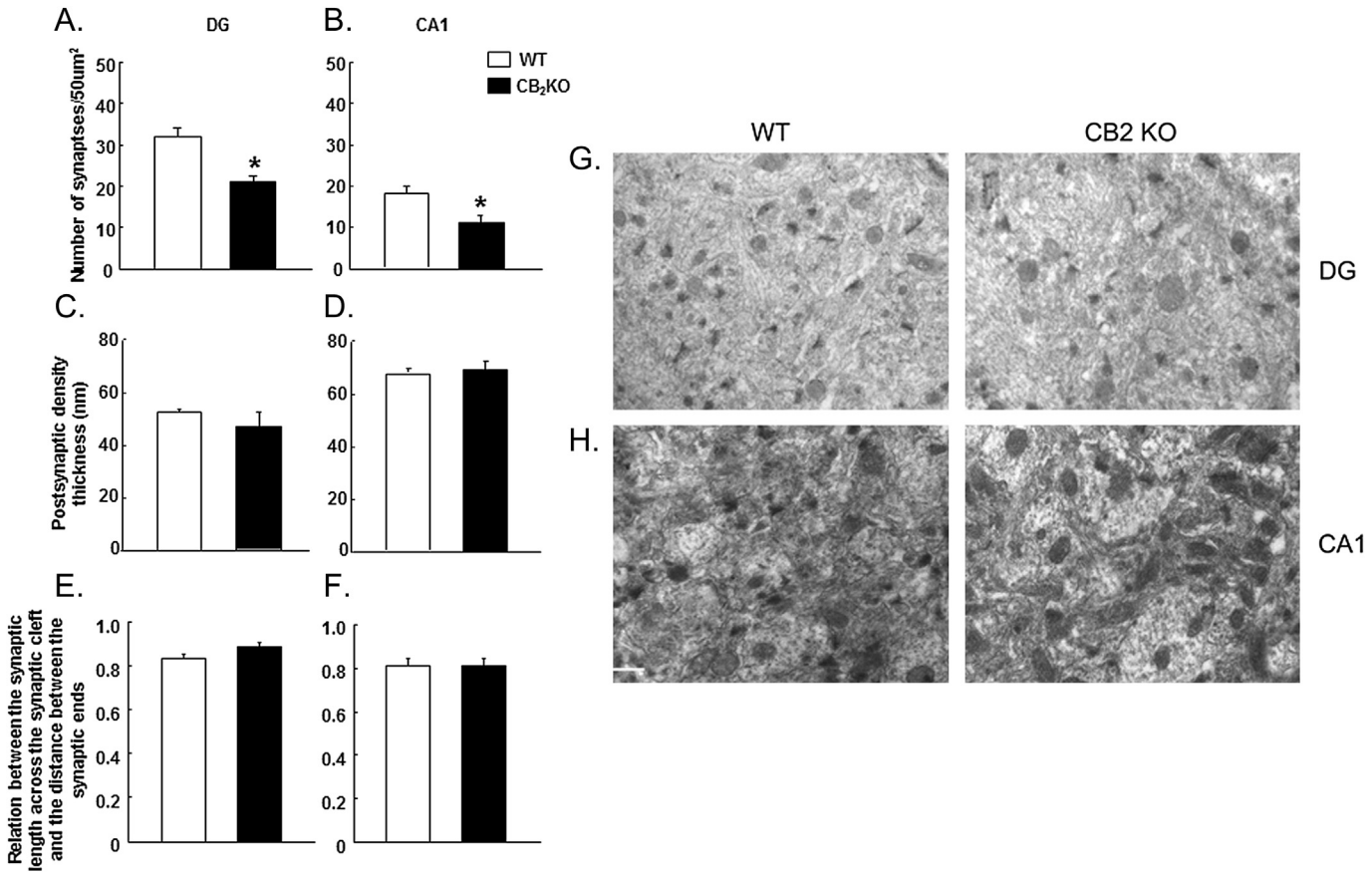

Fig. 3. Electron microscopy analyses in the DG and CA1 fields of HIP from CB2KO and WT mice. Panel A and B: Number of synapses in the DG and CA1 regions. Panel C and D: postsynaptic thickness in the DG and CA1 regions. Panel E and F: Synaptic cleft morphology measured as the relation between the synaptic length across the synaptic cleft and the distances between the synaptic ends in the DG and CA1 regions. Panel G and H: electron microscopy images in CA1 and DG. Data are expressed as mean ± S.E.M. *, Values that are significantly ($p < 0.05$) different from their control group. Scale bars are included in each image.

3.6. Dose–response effects of acute AM630 or JWH133 administration on SDIA test

No difference was observed in training session between the different groups. The results revealed that acute administration of AM630 (1 and 2 mg kg^{-1}) failed to produce any modification. Interestingly, the administration of AM630, at 3 mg kg^{-1} doses, reduced the latency at 1 and 24 h (Two way ANOVA RM followed by Student's Newman Keuls test: treatment $F_{(3,95)} = 2.970$, $p = 0.049$; time $F_{(2,95)} = 59.912$, $p < 0.001$; treatment × time $F_{(6,95)} = 1.969$, $p = 0.086$) ($n = 8–9$/group) (Fig. 5A).

Acute administration of JWH133 failed to produce any modification at 0.5 and 1 mg kg^{-1} doses. In contrast, an increase in latency at 1 and 24 h was observed in WT mice treated with JWH133 (2 mg kg^{-1}). No difference was observed in training session between the different groups (Two way ANOVA RM followed by Student's Newman Keuls test: treatment $F_{(3,95)} = 6.095$, $p = 0.003$; time $F_{(2,95)} = 80.331$, $p < 0.001$; treatment × time $F_{(6,95)} = 2.398$, $p = 0.039$) ($n = 8–9$/group) (Fig. 5B).

4. Discussion

The results of this study support the involvement of CB_2r in memory consolidation, suggesting that this receptor could represent a promising target for developing novel treatments for different cognitive impairment-related disorders. This assumption is supported by the following evidence: 1) the cognitive impairment observed in CB2KO mice in the SDIA, 2) the morphological alterations (MAP2, NF200, SYN, number of synapsis) observed in the HIP of CB2KO mice, 3) the reduced BDNF and NR3C1 gene expression in the HIP of CB2KO mice, 4) the alterations of mTOR/p70S6K signaling cascade (p-p70S6K (T389 and S424) and p-AKT) observed in the PFC and HIP of CB2KO mice, and 4) the cognitive enhancement induced by JWH133.

Previous studies evaluating the role of CB_2r in psychiatric disorders revealed their implication in the response to stress, anxiety, mood and schizophrenia-like disorders (García-Gutiérrez et al., 2010; García-Gutiérrez and Manzanares, 2011; Ortega-Álvaro et al., 2011; Onaivi et al., 2008). The overexpression of CB_2r has been associated with increased resistance to anxiogenic and/or depressogenic-like stimuli (García-Gutiérrez et al., 2010; García-Gutiérrez and Manzanares, 2011). In contrast, the lack of CB_2r was closely related to increased vulnerability to stressful stimuli, mood-related alterations, PPI deficits and cognitive impairment (Ortega-Álvaro et al., 2011).

Despite these results, very little is known about the role of CB_2r in cognitive-related disorders. The aim of this study was to further evaluate the implication of CB_2r in memory acquisition and long-term memory by using CB2KO mice. The lack of CB_2r resulted in a cognitive impairment in short (1 h) and long-term memories (24 h) in the SDIA. Considering that memory disturbances are closely related to the morphological, structural and functional alterations in HIP neuronal circuitry (Scheff et al., 2007), different immunohistological analyses were studied in the HIP of CB2KO

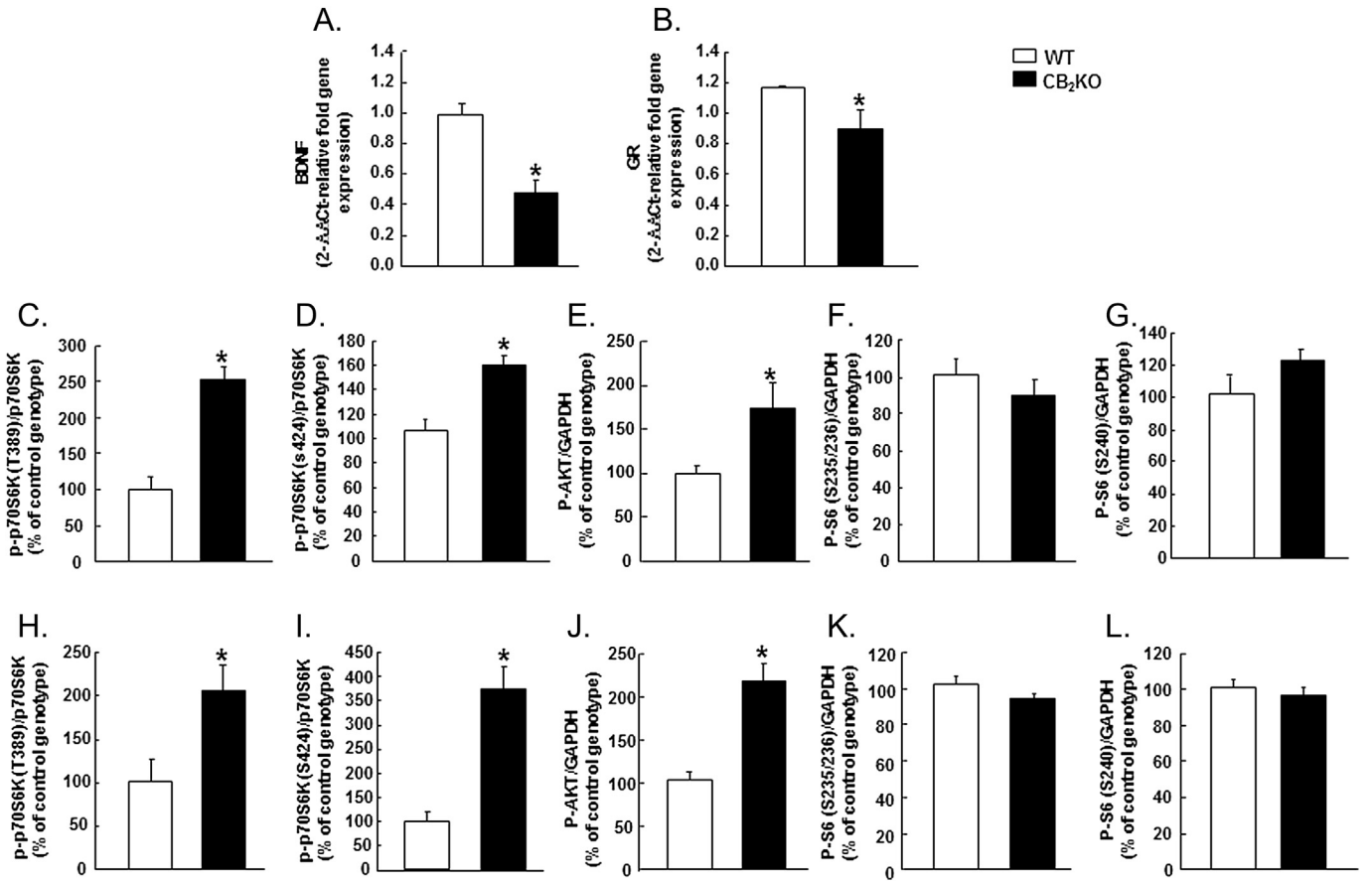

Fig. 4. Evaluation of relative BDNF (A) and NR3C1 gene expression (B) and mTOR pathway (C–J) in PFC and HIP from CB2KO and WT mice. Panel A: Relative BDNF gene expression in the HIP of CB2KO and WT mice. Panel B: Relative NR3C1 gene expression in the HIP of CB2KO and WT mice. Panel C–E: Optical density quantification of the immunoreactive bands for phospho-p70S6K (T389) (C), phospho-p70S6K (S424) (D), AKT (E), S6 (S235/236) (F) and S6 (S240) (G) in the PFC of CB2KO and WT mice. Panel H–L: Optical density quantification of the immunoreactive bands for phospho-p70S6K (T389) (H), phospho-p70S6K (S424) (I), AKT (J), S6 (S235/236) (K) and S6 (S240) (L) in the HIP of CB2KO and WT mice. p70S6K (T389) phosphorylation was measured by immunoblot as a read-out of mTOR activity. Data are expressed as mean ± S.E.M. *, Values that are significantly ($p < 0.05$) different from their control group.

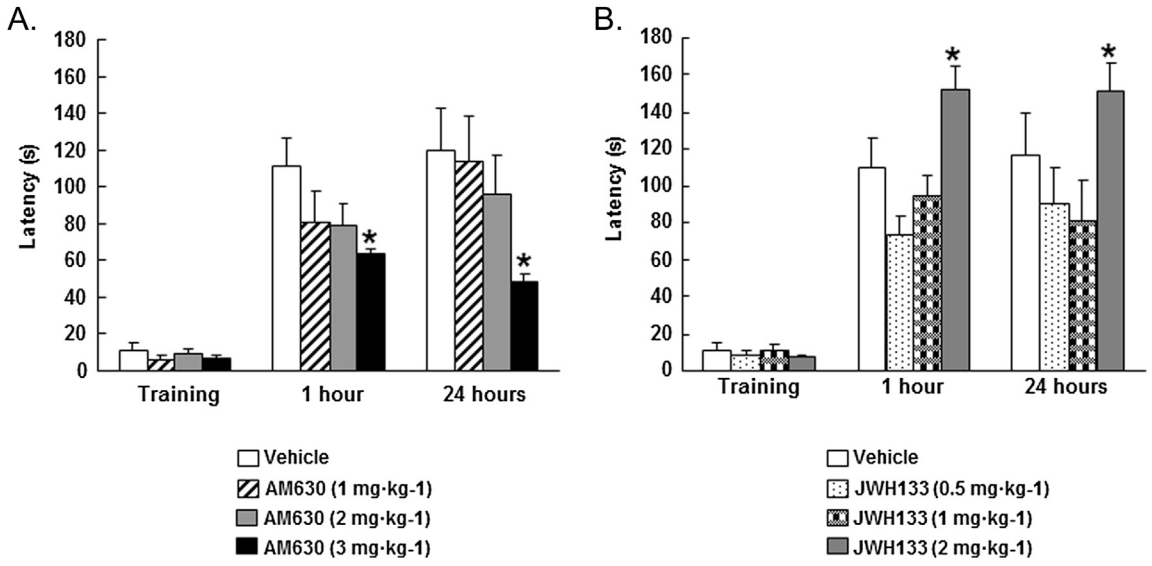

Fig. 5. Dose-response effects of acute AM630 (1, 2 or 3 mg kg^{-1}, ip) (A) or JWH133 (0.5, 1 or 2 mg kg^{-1}, i.p.) (B) administration on step-down inhibitory avoidance test. AM630 or JWH133 was administered immediately after a scrambled foot shock (0.5 mA for 2 s) and the latency was evaluated 1 h (short term memory) and 24 h (long-term memory) later. Columns represent the mean and vertical lines ± SEM of latency (s). *, Values that are significantly ($p < 0.05$) different from their control group.

mice. A reduction in MAP2, NF200, SYN protein expression and in the number of synapses was observed in the DG and CA1 fields of the HIP of CB2KO. The neurofilament NF200 and the neuron-specific cytoskeletal protein MAP2 play a role in the stabilization and maturation of pre-existing connections (Penzes et al., 2009) and in neurogenesis (Dehmelt and Halpain, 2005), respectively. Therefore, the alterations of these parameters, together with the reduction of the 38-kDa Ca^{+2}-binding glycoprotein SYN and the number of synapses, support the existence of abnormalities in the dendritic reorganization and in the synaptic connections in the HIP of CB2KO mice. These morphological alterations may result in the abnormalities in synapse functioning that may underlie the cognitive deficits observed in CB2KO mice. Interestingly, converging evidence confirms a close relation between disturbances in dendritic reorganization and/or synaptic reductions, and impairments of the physiological processes involved in learning and memory (Fanara et al., 2010; (Masliah et al., 1994). Taken together, these alterations further support the existence of morphological disturbances in the synapse remodeling and neurogenesis processes that may underlie the cognitive impairments observed in CB2KO mice.

Furthermore, specific alterations in the BDNF were examined in the HIP of CB2KO mice. One of the main neurotrophic factors involved in neurogenesis is the BDNF, which plays an essential role in modulating the plasticity of adult neurons and glia cells (Huang and Reichardt, 2001), as well as in long-term potentiation (LTP) (Korte et al., 1995) and long-term memory (LTM)(Bekinschtein et al., 2007). BDNF knockout mice (BDNF−/−) presented impairments in learning and memory (Korte et al., 1995). Indeed, blockade of BDNF synthesis using antisense oligonucleotides in rats also interfered with memory retention and inhibited LTP in the HIP (Ma et al., 1998). Interestingly, our results revealed that CB2KO mice presented a significant reduction of BDNF gene expression in the HIP. Accordingly, previous studies revealed that CB2xP mice presented increased BDNF gene expression in the HIP (García-Gutiérrez et al., 2010). Taken together, these results strongly suggest that CB_2r may play an important role in regulating BDNF gene expression.

In order to further explore the mechanism underlying the alterations of the observed BDNF, we examined the gene expression of the glucocorticoid receptor (GR) due to its influence on the regulation of BDNF gene expression (Smith et al., 1995). Previous studies revealed that chronic activation of GR impaired the function and gene expression of CREB (cAMP response element-binding); the main key modulator of BDNF gene expression (Smith et al., 1995). Therefore, chronic activation of GR resulted in a reduction of BDNF gene expression and, consequently, in a reduction of neurogenesis (Cazakoff and Howland, 2010). The results of the present study revealed that CB2KO significantly reduced NR3C1 gene expression in the HIP. Thus, these results supported the fact that the lack of CB_2r (CB2KO) may induce alterations to NR3C1 that may cause changes in BDNF gene expression, and therefore alter the neurogenesis processes. Additional studies are needed to clarify the nature of the molecular alterations observed in CB2KO mice.

The functional relevance of BDNF in long-lasting forms of synaptic plasticity and memory neuroplasticity is partially due to its ability to increase protein synthesis (Sutton and Schuman, 2005; Takei et al., 2004, 2001; Tanaka et al., 2008). Through the activation of its TrkB tyrosine kinase receptor, BDNF stimulates the activation of several signaling pathways, including the PI3K/Akt signaling pathway, to enhance neuronal protein synthesis. This effect, related to the TrkB-dependent activation of the mTOR which induces the phosphorylation of the p70S6K on T389 and T421/S424 (Zhou et al., 2010). p70S6K, is a direct modulator of the ribosomal protein S6 (Lehman et al., 2003) whose phosphorylation state correlates with translational rates. The protein synthesis underlying activity-dependent synaptic plasticity is critically controlled at translation level (Richter and Klann, 2009). In the present study, the phosphorylation of p70S6K on T389 and on S424 was evaluated in the PFC and HIP of CB2KO mice. Indeed, the phosphorylation of AKT was also enhanced in both regions. The increase phosphorylation of both factors has been associated with the cognitive impairments induced by the administration of Δ^9-THC (Puighermanal et al., 2009). Indeed, recent reports proposed that other long-term memory deficits can be associated with an overactivation of the mTOR signaling pathway and an imbalance in protein synthesis. These changes may result in alterations of the translational protein process that may underlie, at least in part, the cognitive impairments observed in CB2KO mice. Recent studies revealed that CB_2r are expressed not only in microglia or astrocytes, but also in neurons (Van Sickle et al., 2005; Gong et al., 2006; Onaivi, 2006; García-Gutiérrez et al., 2010; Aracil-Fernández et al., 2012; Den Boon et al., 2012). It is possible that the effects observed in CB2KO mice may be due to the effects of CB_2r located in microglia, astrocytes and neurons. Further studies are needed to establish the exact mechanism.

If the lack of CB_2r results in molecular adaptations that are associated with cognitive impairments, it can be hypothesized that pharmacological manipulation of CB_2r could produce similar effects in WT mice. To this aim, the SDIA was performed to assess whether the pharmacological modulation of CB_2r by acute administration of the CB_2r-agonist JWH133 or CB_2r-antagonist AM630 would produce changes in cognitive function. Pharmacological blockade of CB_2r resulted in an impairment of short (1 h) and long-term memory (24 h) consolidation. Interestingly, the activation of CB_2r by JWH133 produced a cognitive enhancement of short (1 h) and long-term memory (24 h). In order to further investigate the relative specificity of CB_2r in the mechanism underlying the cognitive alterations of AM630 or JWH133, the effects of both drugs were studied in CB_2KO mice. No effects were observed (Supplemental figure). These results support the involvement of CB_2r as the target involved in the acute effects of JWH133 and AM630 on cognition. The present results coincide with recent studies in which the activation of CB_2r restored synaptic plasticity, cognition and memory impairments induced by bilateral microinjection of amyloid-β $(A\beta)_{1-40}$ fibrils into the hippocampal CA1 area of rats (Wu et al., 2012). Although the precise mechanism underlying these changes remains to be elucidated, it is tempting to speculate that pharmacological CB_2r manipulation may produce alterations in different key elements underlying short and long term memory (BDNF, protein synthesis, glutamate and GABA signaling). It is interesting to note that recent studies have pointed out the participation of CB_2r in the regulation of ERK1/2 and AMPK-CREB pathways, both of which are closely related to the control of memory functions (Franklin and Carrasco, 2013; Choi et al., 2013). Indeed, pharmacological activation of CB_2r by the CB_2r agonist JWH133 (50 nM) resulted in a suppression of GABAergic inhibitory signaling in the entorhinal cortexhippocampal slices (Morgan et al., 2009). Furthermore, the systemic administration of CB_2r agonist MDA-7 significantly ameliorated the impaired basal glutamatergic strength and electric stimuli-induced synaptic plasticity in the hippocampal CA1 area and the memory deficiency induced by the local microinjection of Aβ1− 40 fibrils (Wu et al., 2012). Taken together, these results suggest that the enhanced cognitive function induced by JWH133 may be due to modifications, at least in part, to different key elements which are responsible for memory functions, like ERK1/2, AMPK-CREB, GABA and/or glutamate signaling. Further studies are needed to identify the precise neurochemical mechanisms.

5. Conclusion

In summary, the results presented here show that the CB_2r play a pivotal role in the neurobiology of cognitive process. The lack of CB_2r resulted in an impairment of short and long-term memory processes associated with the alterations of different targets involved in the neuroplasticity of the HIP, such as MAP2, NF200, SYN, BDNF and GR. Furthermore, the increased phosphorylation of proteins involved in the mTOR signaling pathway revealed potential alterations in the translational process that controls the protein synthesis underlying synaptic neuronal plasticity and memory. In addition, acute administration of JWH133 resulted in an enhancement of cognitive function. Taken together, these findings strongly support the role of CB_2r in the regulation of memory and point to this receptor as a potential new target for the treatment of cognitive impairment-related disorders.

Conflict of interest

Non declared.

Contributors

María S. García-Gutiérrez and Antonio Ortega-Álvaro designed the study and wrote the protocol, wrote the first draft of the manuscript, managed the literature searches and analyses, and undertook the statistical analyses. Jose M. Pérez-Ortiz undertook the behavioral studies and the statistical analyses. Authors Laura Caltana, María Jimena Ricatti and Alicia Brusco designed and undertook the histological analyses. Arnau Busquets designed and undertook the analyses of the mTOR pathway. Rafael Maldonado and Jorge Manzanares designed the study, wrote the protocol and revised the first draft of the manuscript. All authors contributed to and have approved the final manuscript.

Acknowledgments

This research was supported by grants from Ministry of Science and Innovation (SAF 2008-01106 and RETICS RD06/0001/1004), Ministry of Health (PNSD 2007/061) and “Red Temática de Investigación Cooperativa en Salud” (RETICS, Instituto de Salud Carlos III, MICINN and FEDER, Madrid, Spain, “Red de Trastornos Adictivos”, RD06/0001/1004) to JM, and Grant UBACYT 00093 (to AB). JMP-O is a postdoctoral fellow supported by FISCAM (Fundación para la investigación sanitaria en Castilla La Mancha). MSG-G is a predoctoral fellow of the Ministry of Science and Innovation. We thank Patricia Rodríguez, Analía Rico and Raquel Poveda for their excellent technical assistance.

Appendix A. Supplementary data

Supplementary data related to this article can be found at http://dx.doi.org/10.1016/j.neuropharm.2013.05.034.

References

Aracil-Fernández, A., Trigo, J.M., García-Gutiérrez, M.S., Ortega-Álvaro, A., Ternianov, A., Navarro, D., et al., 2012. Decreased cocaine motor sensitization and self-administration in mice overexpressing cannabinoid CB_2 receptors. Neuropsychopharmacology 37, 1749–1763.

Atwood, B.K., Mackie, K., 2010. CB2: a cannabinoid receptor with an identity crisis. Br. J. Pharmacol. 160, 467–479.

Baek, J.H., Darlington, C.L., Smith, P.F., Ashton, J.C., 2013. Antibody testing for brain immunohistochemistry: brain immunolabeling for the cannabinoid CB2 receptor. J. Neurosci. Methods 216 (2), 87–95.

Bekinschtein, P., Cammarota, M., Igaz, L.M., et al., 2007. Persistence of long-term memory storage requires a late protein synthesis- and BDNF-dependent phase in the hippocampus. Neuron 53, 261–277.

Breivogel, C.S., Griffin, G., Di Marzo, V., Martin, B.R., 2001. Evidence for a new G protein-coupled cannabinoid receptor in mouse brain. Mol. Pharmacol. 60, 155–163.

Caltana, L., Merelli, A., Lazarowski, A., Brusco, A., 2009. Neuronal and glial alterations due to focal cortical hypoxia induced by direct cobalt chloride ($CoCl_2$) brain injection. Neurotox. Res. 15, 348–358.

Cazakoff, B.N., Howland, J.G., 2010. Acute stress disrupts paired pulse facilitation and long-term potentiation in rat dorsal hippocampus through activation of glucocorticoid receptors. Hippocampus 20, 1327–1331.

Choi, I.-Y., Ju, C., Anthony Jalin, M.A., Lee, D.I., Prather, P.L., et al., 2013. Activation of cannabinoid CB2 receptors mediated AMPK/CREB pathway reduces cerebral ischemic injury. Am. J. Pathol. 182, 928–939.

Costanzi, M., Battaglia, M., Rossi-Arnaud, C., Cestari, V., Castellano, C., 2004. Effects of anandamide and morphine combinations on memory consolidation in cd1 mice: involvement of dopaminergic mechanisms. Neurobiol. Learn. Mem. 81, 144–149.

Da, S., Takahashi, R.N., 2002. SR 141716A prevents delta 9-tetrahydrocannabinol-induced spatial learning deficit in a Morris-type water maze in mice. Prog. Neuropsychopharmacol. Biol. Psychiatry 26, 321–325.

Dehmelt, L., Halpain, S., 2005. The MAP2/Tau family of microtubule-associated proteins. Genome Biol. 6, 204.

Den Boon, F.S., Chameau, P., Schaafsma-Zhao, Q., van Aken, W., Bari, M., Oddi, S., et al., 2012. Excitability of prefrontal cortical pyramidal neurons is modulated by activation of intracellular type-2 cannabinoid receptors. Proc. Natl. Acad. Sci. U. S. A. 109 (9), 3534–3539.

Fanara, P., Husted, K.H., Selle, K., Wong, P.Y., Banerjee, J., Brandt, R., et al., 2010. Changes in microtubule turnover accompany synaptic plasticity and memory formation in response to contextual fear conditioning in mice. Neuroscience 168, 167–178.

Franklin, J.M., Carrasco, G.A., 2013. Cannabinoid receptor agonists upregulate and enhance serotonin 2A (5-HT(2A)) receptor activity via ERK1/2 signaling. Synapse 67 (3), 145–159.

García-Gutiérrez, M.S., Manzanares, J., 2011. Overexpression of CB2 cannabinoid receptors decreased vulnerability to anxiety and impaired anxiolytic action of alprazolam in mice. J. Psychopharmacol. 25, 111–120.

García-Gutiérrez, M.S., Pérez-Ortiz, J.M., Gutiérrez-Adán, A., Manzanares, J., 2010. Depression-resistant endophenotype in mice overexpressing cannabinoid CB(2) receptors. Br. J. Pharmacol. 160, 1773–1784.

Gong, J.P., Onaivi, E.S., Ishiguro, H., Liu, Q.R., Tagliaferro, P.A., Brusco, A., et al., 2006. Cannabinoid CB2 receptors: immunohistochemical localization in rat brain. Brain Res. 1071, 10–23.

Griffin, G., Wray, E.J., Tao, Q., McAllister, S.D., Rorrer, W.K., Aung, M.M., Martin, B.R., Abood, M.E., 1999. Evaluation of the cannabinoid CB2 receptor-selective antagonist, SR144528: further evidence for cannabinoid CB2 receptor absence in the rat central nervous system. Eur. J. Pharmacol. 377 (1), 117–125.

Hajos, N., Ledent, C., Freund, T.F., 2001. Novel cannabinoid-sensitive receptor mediates inhibition of glutamatergic synaptic transmission in the hippocampus. Neuroscience 106, 1–4.

Herkenham, M., Lynn, A.B., Johnson, M.R., Melvin, L.S., de Costa, B.R., Rice, K.C., 1991. Characterization and localization of cannabinoid receptors in rat brain: a quantitative in vitro autoradiographic study. J. Neurosci. 11, 563–583.

Huang, E.J., Reichardt, L.F., 2001. Neurotrophins: roles in neuronal development and function. Annu. Rev. Neurosci. 24, 677–736.

Huffman, J.W., Liddle, J., Yu, S., Aung, M.M., Abood, M.E., Wiley, J.L., et al., 1999. 3-(1',1'-Dimethylbutyl)-1-deoxy-delta8-THC and related compounds: synthesis of selective ligands for the CB2 receptor. Bioorg. Med. Chem. 7, 2905–2914.

Kofalvi, A., Vizi, E.S., Ledent, C., Sperlagh, B., 2003. Cannabinoids inhibit the release of [3H]glutamate from rodent hippocampal synaptosomes via a novel CB1 receptor-independent action. Eur. J. Neurosci. 18, 1973–1978.

Korte, M., Carroll, P., Wolf, E., Brem, G., Thoenen, H., Bonhoeffer, T., 1995. Hippocampal long-term potentiation is impaired in mice lacking brain-derived neurotrophic factor. Proc. Natl. Acad. Sci. U. S. A. 92, 8856–8860.

Lehman, J.A., Calvo, V., Gomez-Cambronero, J., 2003. Mechanism of ribosomal p70S6 kinase activation by granulocyte macrophage colony-stimulating factor in neutrophils: cooperation of a MEK-related, THR421/SER424 kinase and a rapamycin-sensitive, m-TOR-related THR389 kinase. J. Biol. Chem. 278, 28130–28138.

Livak, K.J., Schmittgen, T.D., 2001. Analysis of relative gene expression data using real-time quantitative PCR and the 2(-Delta Delta C(T)) Method. Methods 25, 402–408.

Ma, Y.L., Wang, H.L., Wu, H.C., Wei, C.L., Lee, E.H., 1998. Brain-derived neurotrophic factor antisense oligonucleotide impairs memory retention and inhibits long-term potentiation in rats. Neuroscience 82, 957–967.

Masliah, E., Mallory, M., Hansen, L., DeTeresa, R., Alford, M., Terry, R., 1994. Synaptic and neuritic alterations during the progression of Alzheimer's disease. Neurosci. Lett. 174, 67–72.

Mishima, K., Egashira, N., Hirosawa, N., Fujii, M., Matsumoto, Y., Iwasaki, K., et al., 2001. Characteristics of learning and memory impairment induced by delta9-tetrahydrocannabinol in rats. Jpn. J. Pharmacol. 87, 297–308.

Morgan, N.H., Stanford, I.M., Woodhall, G.L., 2009. Functional CB2 type cannabinoid receptors at CNS synapses. Neuropharmacology 57, 356–368.

Onaivi, E.S., 2006. Neuropsychobiological evidence for the functional presence and expression of cannabinoid CB2 receptors in the brain. Neuropsychobiology 54, 231–246.

Onaivi, E.S., Ishiguro, H., Gong, J.P., Patel, S., Meozzi, P.A., Myers, L., et al., 2008. Brain neuronal CB2 cannabinoid receptors in drug abuse and depression: from mice to human subjects. PLoS ONE 3, e1640.
Ortega-Álvaro, A., Aracil-Fernández, A., García-Gutiérrez, M.S., Navarrete, F., Manzanares, J., 2011. Deletion of CB2 cannabinoid receptor induces schizophrenia-related behaviors in mice. Neuropsychopharmacology 36, 1489–1504.
Palkovits, M., 1983. Punch sampling biopsy technique. Methods Enzymol. 103, 368–376.
Pamplona, F.A., Takahashi, R.N., 2006. WIN 55212-2 impairs contextual fear conditioning through the activation of CB1 cannabinoid receptors. Neurosci. Lett. 397, 88–92.
Paxinos, G., Franklin, K.B.J., 2001. The Mouse Brain in Stereotaxic Coordinates. Academic Press. Harcourt Science and Technology Company, New York.
Penzes, P., Srivastava, D.P., Woolfrey, K.M., 2009. Not just actin? A role for dynamic microtubules in dendritic spines. Neuron 61, 3–5.
Pertwee, R., Griffin, G., Fernando, S., Li, X., Hill, A., Makriyannis, A., 1995. AM630, a competitive cannabinoid receptor antagonist. Life Sci. 56, 1949–1955.
Puighermanal, E., Marsicano, G., Büsquets-García, A., Lutz, B., Maldonado, R., Ozaita, A., 2009. Cannabinoid modulation of hippocampal long-term memory is mediated by mTOR signaling. Nat. Neurosci. 12, 1152–1158.
Reynolds, E.S., 1963. The use of lead citrate at high pH as an electron-opaque stain in electron microscopy. J. Cell. Biol. 17, 208–212.
Richter, J.D., Klann, E., 2009. Making synaptic plasticity and memory last: mechanisms of translational regulation. Genes Dev. 23, 1–11.
Riedel, G., Davies, S.N., 2005. Cannabinoid function in learning, memory and plasticity. Handb. Exp. Pharmacol., 445–477.
Scheff, S.W., Price, D.A., Schmitt, F.A., DeKosky, S.T., Mufson, E.J., 2007. Synaptic alterations in CA1 in mild Alzheimer disease and mild cognitive impairment. Neurology 68, 1501–1508.
Smith, M.A., Makino, S., Kvetnansky, R., Post, R.M., 1995. Stress and glucocorticoids affect the expression of brain-derived neurotrophic factor and neurotrophin-3 mRNAs in the hippocampus. J. Neurosci. 15, 1768–1777.
Sutton, M.A., Schuman, E.M., 2005. Local translational control in dendrites and its role in long-term synaptic plasticity. J. Neurobiol. 64, 116–131.
Tagliaferro, P., Javier Ramos, A., Onaivi, E.S., Evrard, S.G., Lujilde, J., Brusco, A., 2006. Neuronal cytoskeleton and synaptic densities are altered after a chronic treatment with the cannabinoid receptor agonist WIN 55,212-2. Brain Res. 1085, 163–176.
Takei, N., Kawamura, M., Hara, K., et al., 2001. Brain-derived neurotrophic factor enhances neuronal translation by activating multiple initiation processes: comparison with the effects of insulin. J. Biol. Chem. 276, 42818–42825.
Takei, N., Inamura, N., Kawamura, M., et al., 2004. Brain-derived neurotrophic factor induces mammalian target of rapamycin-dependent local activation of translation machinery and protein synthesis in neuronal dendrites. J. Neurosci. 24, 9760–9769.
Tanaka, J., Horiike, Y., Matsuzaki, M., et al., 2008. Protein synthesis and neurotrophin-dependent structural plasticity of single dendritic spines. Science 319, 1683–1687.
Thiemann, G., Fletcher, B.C., Ledent, C., Molleman, A., Hasenohrl, R.U., 2007. The genetic versus pharmacological invalidation of the cannabinoid CB(1) receptor results in differential effects on 'non-associative' memory and forebrain monoamine concentrations in mice. Neurobiol. Learn. Mem. 88, 416–423.
Urigüen, L., Pérez-Rial, S., Ledent, C., Palomo, T., Manzanares, J., 2004. Impaired action of anxiolytic drugs in mice deficient in cannabinoid CB1 receptors. Neuropharmacology 46, 966–973.
Van Sickle, M.D., Duncan, M., Kingsley, P.J., Mouihate, A., Urbani, P., Mackie, K., et al., 2005. Identification and functional characterization of brainstem cannabinoid CB2 receptors. Science 310 (5746), 329–332.
Wu, J., Bie, B., Yang, H., Xu, J.J., Brown, D.L., Naguib, M., 2012. Activation of the CB(2) receptor system reverses amyloid-induced memory deficiency. Neurobiol. Aging 34 (3), 791–804.
Xi, Z.X., Peng, X.Q., Li, X., Song, R., Zhang, H.Y., Liu, Q.R., et al., 2011. Brain cannabinoid CB(2) receptors modulate cocaine's actions in mice. Nat. Neurosci. 14, 1160–1166.
Zhou, X., Lin, D., Zheng, F., et al., 2010. Intracellular calcium and calmodulin link brain-derived neurotrophic factor to p70S6 kinases phosphorylation and dendritic protein synthesis. J. Neurosci. Res. 88, 1420–1432.